ELSEVIER

www.elsevier.nl/locate/ica

Inorganica Chimica Acta 300–302 (2000) 855–861

Inorganica Chimica Acta

Di-μ-halo-bis{[tris(2-pyridylmethyl)amine-κ⁴*N*]nickel(II)} bis(triethylammonium) tetraperchlorate: Magnetostructural studies

Bing Tong [a], Shih-Chi Chang [b], Everett E. Carpenter [c], Charles J. O'Connor [c], Jackson O. Lay Jr. [d], Richard E. Norman [a,*]

[a] *Chemistry Department, CNSB-210, University of Louisiana at Monroe, Monroe, LA 71209, USA*
[b] *Department of Physics, Duquesne University, Pittsburgh, PA 15282, USA*
[c] *Advanced Materials Research Institute, University of New Orleans, New Orleans, LA 70148, USA*
[d] *Division of Chemistry, Food and Drug Administration/National Center for Toxicological Research, Jefferson, AR 72079, USA*

Received 30 November 1999

Abstract

$[\{Ni(TPA)Br\}_2](ClO_4)_2\cdot 2HNEt_3ClO_4$, where TPA is tris-(2-pyridylmethyl)amine, crystallizes in the monoclinic space group $P2_1/c$ with $Z = 2$, $a = 11.531(3)$ Å, $b = 22.141(3)$ Å, $c = 12.511(2)$ Å and $\beta = 107.44(1)°$. The structure was determined at ambient temperature from 5519 reflections (2937 observed) with $R = 0.0426$ and $R_w = 0.0404$. The $[\{Ni(TPA)Br\}_2]^{2+}$ core is centrosymmetric with unsymmetrical bridges (Ni–Br = 2.504(1) and 2.662(1) Å). Each Ni atom is pseudo-octahedral six-coordinate. Triethylammonium perchlorate cocrystallizes with the metal complex. Magnetic susceptibility studies (fit to the Ginsberg model) indicate the Ni centers are ferromagnetically coupled with $J/k = 10.0(5)$ cm^{-1}. The chloro complex ($[\{Ni(TPA)Cl\}_2](ClO_4)_2\cdot 2HNEt_3ClO_4$) is also ferromagnetically coupled with $J/k = 7.6(1)$ cm^{-1}.

Keywords: Crystal structures; Nickel(II) complexes; Magnetic susceptibility; Ferromagnetic coupling

1. Introduction

There is considerable interest in how various superexchange pathways affect magnetic communication between metal centers. One relatively simple system of particular interest is the system with two bridging ligands in a 'diamond' arrangement ($\{ML\}_2$). For Ni(II), when the Ni is five-coordinate, the coupling is usually antiferromagnetic [1]. However, when the Ni is six-coordinate, the situation is more complicated. In cases where there is pronounced tetragonal distortion, the degeneracy of the e_g level is removed and the coupling is antiferromagnetic [2]. In cases where the metal center is octahedral or pseudo-octahedral, the degeneracy of the e_g level is maintained and the coupling is always ferromagnetic [3–8]. For the $[\{Ni(en)Cl\}_2]^{2+}$ series, where en is ethylenediamine, with Cl^-, ClO_4^- and BPh_4^- as the counter ions, the extent of ferromagnetic coupling increases as the Ni–Ni separation decreases and the sum of the Ni–Cl bonds also decreases [5,6,8]. In other words, in this series, the extent of coupling increases as the ferromagnetic superexchange pathlength decreases. When the bridging chlorides are replaced by bromides, good comparisons of the impact of this change on the magnetic properties cannot be made because only one structure with the $\{NiBr\}_2$ core has been determined by single crystal X-ray crystallography [9], and magnetic measurements have not been reported for this compound.

We recently reported the structure $[\{Ni(TPA)Cl\}_2](ClO_4)_2\cdot 2HNEt_3ClO_4$ [10], where TPA is *tris*(2-pyridylmethyl)amine, which contains the $\{NiCl\}_2$ core. We now report the structure of the bromine analog ($[\{Ni(TPA)Br\}_2](ClO_4)_2\cdot 2HNEt_3ClO_4$), the spectral characterization, and the magnetic susceptibility studies of both complexes.

* Corresponding author. Tel.: +1-318-342 1836; fax: +1-318-342 1859.
E-mail address: chnorman@alpha.nlu.edu (R.E. Norman)

0020-1693/00/$ - see front matter
PII: S0020-1693(99)00591-5

2. Experimental

2.1. Synthesis

2.1.1. [{Ni(TPA)Br}$_2$](ClO$_4$)$_2$·2HNEt$_3$ClO$_4$ (1)

TPA·HClO$_4$ (0.1954 g, 0.501 mmol) was dissolved in 20 ml of methanol, followed by the addition of triethylamine (105 μl, 0.75 mmol). Ni(ClO$_4$)$_2$·6H$_2$O (0.1829 g, 0.500 mmol) was added to the resulting solution. HN(CH$_2$CH$_3$)$_3$Br (0.0910 g, 0.500 mmol) was then added. This solution was stirred for 30 min, and then allowed to stand at room temperature covered by parafilm in which a small hole had been punched. After 7 days, sky blue rectangular prismatic crystals of **1** were obtained which were suitable for X-ray analysis. The observed (uncorrected) melting point is 276–280°C. **Caution:** the perchlorate salts in this study are all potentially explosive and should be handled with care.

2.1.2. [{Ni(TPA)Cl}$_2$](ClO$_4$)$_2$·2HNEt$_3$ClO$_4$ (2)

Prepared as previously reported [10].

2.2. Structure determination

Details of the crystal and data collection are collected in Tables 1–3. The cell constants were determined by least-squares refinement on diffractometer angles for 24 automatically centered reflections in the range $20.0 < 2\theta < 26.2°$ using graphite-monochromated Mo Kα radiation ($\lambda = 0.71069$ Å). The data were collected at room temperature using a Rigaku AFC7R diffractometer with a 12 kW rotating anode generator in the ω–2θ mode with θ scan width of $1.10 + 0.35\tan\theta$, ω-scan speed of 16° min^{-1}. Of the 5807 reflections measured to a maximum 2θ value of 50.0°, 2937 were observed (observed criterion $I > 2.00\sigma(I)$). Over the course of data collection, the intensities of three standard reflections decreased by 0.46%. The data were corrected for this decrease and for absorption. The structure was solved using direct methods [11], and expanded using Fourier techniques [12]. Full-matrix least-squares refinement with anisotropic thermal parameters for all of the non-hydrogen atoms converged with $R = \Sigma||F_o| - |F_c||/\Sigma|F_o| = 0.043$ and $R_w[\Sigma w(|F_o| - |F_c|)^2/\Sigma wF_o^2]^{1/2} =$

Table 1
Crystallographic details for [{Ni(TPA)Br}$_2$](ClO$_4$)$_2$·2HNEt$_3$ClO$_4$ (**1**)

Empirical formula	$NiBr_2Cl_4C_{48}H_{68}N_{10}O_{16}$
Formula weight	1460.14
Crystal system	monoclinic
Space group	$P2_1/c$ (no. 14)
Z	2
Unit cell dimensions	
a (Å)	11.531(3)
b (Å)	22.141(3)
c (Å)	12.511(2)
β (°)	107.44(1)
V (Å^3)	3047.3(9)
μ (mm^{-1})	2.18
Crystal size (mm)	$0.30 \times 0.20 \times 0.10$
D_{calc} (g cm^{-3})	1.591
$F(000)$	1496
Radiation (λ, Å)	Mo Kα (0.71069)
2θ Range	3.4–50
h,k,l Collected	13, 26, ±14
Reflections measured	5807
Unique reflections	5519
Reflections observed	2937
Parameters	370
R	0.0426
R_w	0.0404

Table 2
Fractional atomic coordinates for [{Ni(TPA)Br}$_2$](ClO$_4$)$_2$·2HNEt$_3$ClO$_4$ (**1**)

Atom	x	y	z	U_{eq}
Br(1)	0.90009(7)	−0.06347(3)	0.98099(7)	0.0363(2)
Ni(1)	0.86114(8)	0.04795(4)	0.97375(8)	0.0295(3)
N(1)	0.8277(5)	0.1401(2)	0.9718(5)	0.033(2)
N(2)	0.8842(5)	0.0625(3)	1.1425(5)	0.033(2)
N(3)	0.8398(5)	0.0634(3)	0.8046(5)	0.037(2)
N(4)	0.6722(5)	0.0414(3)	0.9271(5)	0.031(2)
C(1)	0.9026(7)	0.1642(3)	1.0819(7)	0.042(3)
C(2)	0.9014(6)	0.1213(3)	1.1738(7)	0.038(3)
C(3)	0.9240(7)	0.1374(4)	1.2844(8)	0.050(3)
C(4)	0.9284(8)	0.0946(5)	1.3646(7)	0.063(4)
C(5)	0.9092(8)	0.0350(4)	1.3329(7)	0.051(3)
C(6)	0.8877(7)	0.0212(3)	1.2211(7)	0.039(3)
C(7)	0.8629(7)	0.1653(4)	0.8764(7)	0.050(3)
C(8)	0.8296(6)	0.1223(3)	0.7780(7)	0.036(3)
C(9)	0.7963(7)	0.1412(4)	0.6683(8)	0.052(3)
C(10)	0.7762(8)	0.1009(5)	0.5844(7)	0.058(3)
C(11)	0.7880(8)	0.0397(4)	0.6113(7)	0.055(3)
C(12)	0.8190(7)	0.0237(3)	0.7217(7)	0.042(3)
C(13)	0.6958(7)	0.1488(3)	0.9595(6)	0.045(3)
C(14)	0.6182(7)	0.0960(3)	0.9132(6)	0.033(2)
C(15)	0.4943(7)	0.1024(3)	0.8638(7)	0.046(3)
C(16)	0.4234(7)	0.0525(4)	0.8302(7)	0.055(3)
C(17)	0.4764(8)	−0.0037(4)	0.8441(7)	0.048(3)
C(18)	0.6022(7)	−0.0069(3)	0.8920(7)	0.043(3)
Cl(1)	0.1213(2)	0.1766(1)	0.6642(2)	0.0601(9)
O(1)	0.2496(5)	0.1872(3)	0.6904(5)	0.076(2)
O(2)	0.1027(7)	0.1162(3)	0.6630(8)	0.151(4)
O(3)	0.0582(6)	0.2002(3)	0.5587(5)	0.099(3)
O(4)	0.0758(6)	0.2065(4)	0.7445(6)	0.142(4)
Cl(2)	0.6046(2)	0.2994(1)	0.7646(2)	0.0543(8)
O(5)	0.6745(6)	0.2806(3)	0.6955(5)	0.083(3)
O(6)	0.5115(5)	0.2561(3)	0.7583(5)	0.077(2)
O(7)	0.5545(7)	0.3548(3)	0.7319(9)	0.172(4)
O(8)	0.6842(7)	0.3006(3)	0.8754(5)	0.099(3)
N(5)	0.3480(6)	0.1954(3)	0.4991(5)	0.049(2)
C(19)	0.3760(8)	0.2591(4)	0.4749(8)	0.059(3)
C(20)	0.2912(9)	0.3046(4)	0.4967(8)	0.076(4)
C(21)	0.4604(8)	0.1577(4)	0.5261(7)	0.066(3)
C(22)	0.4391(9)	0.0931(5)	0.5530(9)	0.093(4)
C(23)	0.2416(7)	0.1691(4)	0.4089(8)	0.058(3)
C(24)	0.2672(9)	0.1565(4)	0.3010(7)	0.071(4)

Table 3
Chemical bond distances (Å) and angles (°) for the coordination sphere of $[\{Ni(TPA)Br\}_2](ClO_4)_2 \cdot 2HNEt_3ClO_4$ (**1**)

Br(1)–Ni(1)	2.504(1)
Br(1)–Ni(1)*	2.662(1)
Ni(1)–N(1)	2.075(5)
Ni(1)–N(2)	2.072(5)
Ni(1)–N(3)	2.084(6)
Ni(1)–N(4)	2.084(6)
Ni(1)–Br(1)–Ni(1)*	92.49(4)
Br(1)–Ni(1)–Br(1)*	87.51(4)
Br(1)–Ni(1)–N(1)	178.4(2)
Br(1)–Ni(1)–N(2)	98.6(2)
Br(1)–Ni(1)–N(3)	99.4(2)
Br(1)–Ni(1)–N(4)	95.9(2)
Br(1)*–Ni(1)–N(1)	93.0(2)
Br(1)*–Ni(1)–N(2)	87.4(1)
Br(1)*–Ni(1)–N(3)	89.7(2)
Br(1)*–Ni(1)–N(4)	174.9(2)
N(1)–Ni(1)–N(2)	80.0(2)
N(1)–Ni(1)–N(3)	82.0(2)
N(1)–Ni(1)–N(4)	83.7(2)
N(2)–Ni(1)–N(3)	161.6(2)
N(2)–Ni(1)–N(4)	95.8(2)
N(3)–Ni(1)–N(4)	86.1(2)

0.040. The function minimized in refinement was $\Sigma w(|F_o| - |F_c|)^2$ where $w = 1/[\sigma^2(F_o) + 0.00002|F_o|^2]$. H atoms were placed in idealized positions (C–H 0.95 Å and N–H 0.97 Å), with $U_{iso} = 1.2U_{eq}$ of the attached atom. Neutral atom scattering factors were taken from Cromer and Waber [13]. Anomalous dispersion effects were included in F_c [14], and the values for $\Delta f'$ and $\Delta f''$ were those of Creagh and McAuley [15]. The values for the mass attenuation coefficients were those of Creagh and Hubbell [16]. All calculations were performed using the teXsan [17] crystallographic software package. The atomic numbering scheme is shown in Fig. 1.

2.3. Other physical methods

Magnetic susceptibility data were recorded over a temperature range of 1.8–300 K at a measuring field of 100 Oe with a Quantum Design MPMS-5 SQUID susceptometer. Calibration and operating procedures have been reported elsewhere [18]. The data were corrected for the diamagnetic contribution of the sample holder and the diamagnetism of the sample using Pascal's constants [18].

Mass spectral samples were dissolved in acetonitrile for flow injection analysis electrospray ionization mass spectrometry using a Finnigan TSQ7000. Samples (10 μl) were injected into a sample loop, and flow injection was accomplished using 100 μl min^{-1} of 50% by volume aqueous acetonitrile (with 0.1% formic acid). The ESI voltage was 4.5 keV and the capillary temperature was 200°C. For **1**, key clusters of peaks were observed at m/z of 429, 891, 937, 957 and 975. For **2**, key clusters of peaks were observed at m/z of 383, 803, 867 and 931. Isotope patterns calculated using the 'Isoform' program for the assignments given below, gave excellent fits to the observed patterns.

Electronic spectra were recorded on a Hitachi Model U-2000 at Louisiana Tech University and ^1H NMR spectra were recorded at ambient temperature on a JEOL EX/400 at 400 MHz. Chemical shifts were referenced to the proton signal of CD_2HCN. The acquisition conditions were 6.8 μs pulses, 8192 data points,

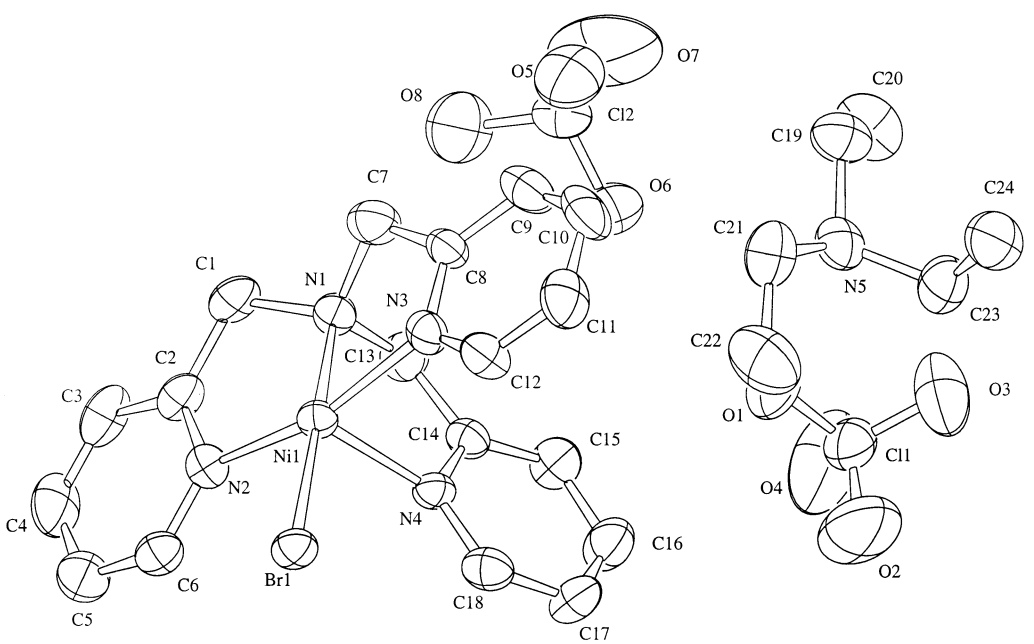

Fig. 1. Perspective drawing of the asymmetric unit of $[\{Ni(TPA)Br\}_2](ClO_4)_2 \cdot 2HNEt_3ClO_4$ (**1**) showing the atom numbering scheme. Ellipsoids are drawn at 50% probability.

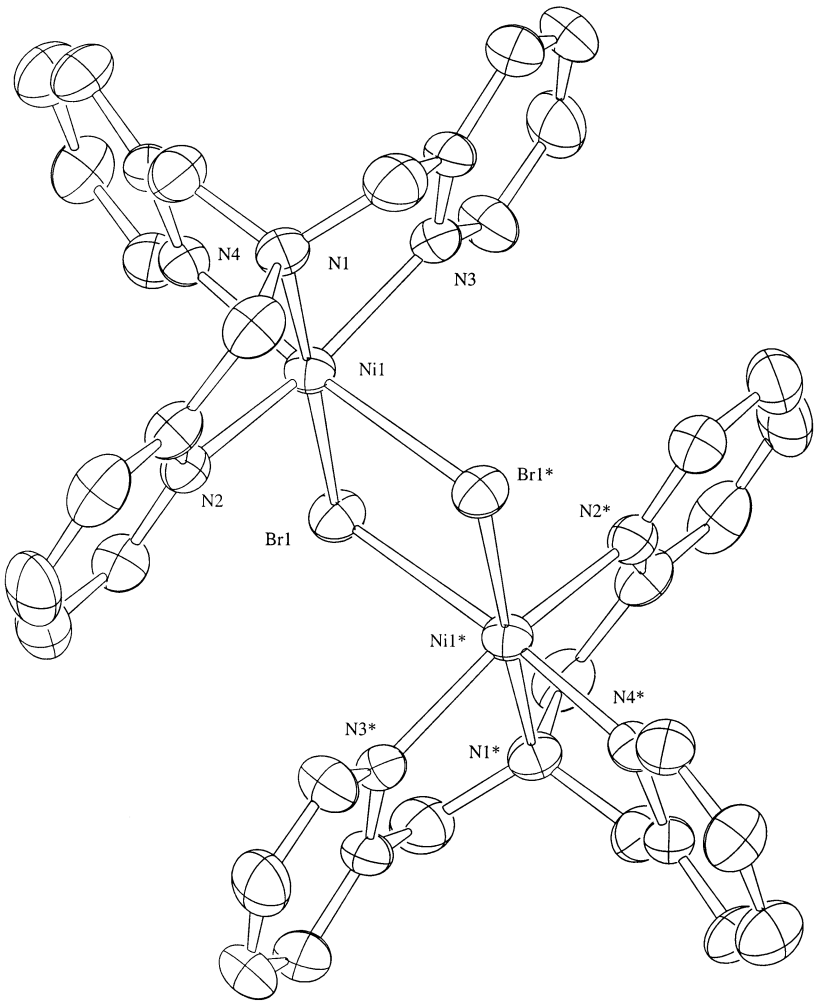

Fig. 2. Perspective drawing of the dimeric dication $[\{Ni(TPA)Br\}_2]^{2+}$ of **1**. Ellipsoids are drawn at 50% probability.

200 kHz scan width, 41 ms acquisition time, and typically 10 000 scans.

3. Results and discussion

3.1. Solid state structure

The structure of **1** is very similar to the analogous Cl structure (**2**) recently reported [10], and consists of two triethylammonium ions, four perchlorates and a nickel dimer bridged by two bromides, as shown in Figs. 1 and 2. The metrical parameters of the triethylammonium ion and perchlorate ions are unremarkable (Supplementary material) and the triethylammonium ion hydrogen bonds to a perchlorate; the separation of O1 (a perchlorate oxygen) to N5 (the triethylammonium nitrogen) is 2.945(8) Å. The nickel dimer consists of a centrosymmetric unit of two Ni atoms bridged unsymmetrically by two Br atoms, as shown in Fig. 2. The separation of the two Ni atoms is 3.733(1) Å, and the Br–Br separation is 3.575(1) Å. The Ni atoms are pseudo-octahedral six-coordinate, with four N atoms from the TPA ligand completing the coordination environment. The Ni–Br distances (2.504(1) and 2.662(1) Å) differ by 0.158 Å. The shorter Ni–Br distance is *trans* to the tertiary amine of TPA again reflecting the lower Lewis basicity of the tertiary amine relative to the pyridine [10]. The sum of the Ni–Br distances (the ferromagnetic superexchange pathlength) is 5.166 Å. There have only been two other single crystal X-ray structures reported containing six-coordinate Ni(II) and the $\{NiBr\}_2$ core, namely $Ni(en)_2Br_2$ [19] and $NiBr_2{\cdot}4EtOH$ [9]. In $Ni(en)_2Br_2$, the reported structure is low resolution (the Ni–Br distance given is 2.7 Å), and the compound is stated to be isomorphous to the Cl analog [19]. The Cl analog structure has been subsequently redetermined twice [5,20] and in both cases, the Ni–Cl bridges were asymmetric. Thus, it is expected that the Br analog also contains asymmetric Ni–Br bridges. In $NiBr_2{\cdot}4EtOH$, the Ni–Br bridges are slightly asymmetric (2.525(3) and 2.556(3) Å yielding a ferromagnetic superexchange pathlength of 5.081 Å), and the Ni separation is 3.624(2) Å while the Br–Br separa-

tion is 3.562(4) Å [9]. Additionally, there have been three reports of structures determined by powder diffraction [21–23]. All of these compounds have the form NiL_2Br_2 forming polymeric structures with bridging bromides. Thus each Ni has four bromide bridges to two other Ni centers. The Ni–Br distances range from 2.560(2) to 2.631(8) Å, one has a very short Ni separation of 3.401 Å, while the other two have values of 3.733 and 3.771 Å. So, in comparison, **1** exhibits 'typical' Ni–Ni separations, fairly asymmetric Ni–Br bridges, and typical ferromagnetic superexchange pathways.

The magnetic susceptibility data from 180 to 300 K for each compound were fit to a Curie–Weiss law with $C = 1.090$ and 0.980 for **2** and **1**, respectively. Using these values, g-values were determined which were held constant while fitting the low temperature data using the Ginsberg model [3] based upon the spin Hamiltonian

$$\mathscr{H} = -2JS_1 \cdot S_2 - D(S_{1z}^2 + S_{2z}^2) - g\mu_\beta H \cdot (S_1 + S_2) - Z'J'S\langle S\rangle$$

in which the symbols have their usual meaning. J denotes the isotropic intradimer exchange interaction, D the axial zero-field splitting, and $Z'J'$ the interdimer exchange interaction. The best fits were, for **2**, $J/k =$ 7.6(1) cm^{-1}, $g = 2.07$, $D/k = 0.51$ cm^{-1} and $Z'J'/k =$ 0.11 cm^{-1}; and, for **1**, $J/k = 10.0(5)$ cm^{-1}, $g = 2.34$, $D/k = 1.22$ cm^{-1} and $Z'J'/k = 0.06$ cm^{-1}. Notably these nickel dimers are ferromagnetically coupled with the bromide dimer more strongly coupled than the chloride dimer. These values are collected in Table 4 and compared to previously reported values. The J value for the chloride dimer is near the low end of the range of values in the literature, however the ferromagnetic superexchange pathway is the second shortest reported for these compounds. It had been suggested that the decrease in the ferromagnetic superexchange pathway could be the main cause of the increase in the ferromagnetic coupling for the $[\{Ni(en)_2Cl\}_2]^{2+}$ series [8], but the magnetic susceptibility data for **2** indicates that it may not be so simple. Similarly, for Fe(III) dimers bridged by a ligand oxygen atom and at least one other bridging ligand, a correlation was found between the superexchange pathway length (antiferromagnetic for these cases) and the coupling constant—the shorter the separation, the larger the coupling [25]. In the Fe(III) case, the quantitative correlation was based on 36 magnetostructural observations [25], yet for these Ni(II) complexes only eight examples have been reported. Clearly more examples are needed for Ni(II). While it is premature to speculate upon the differences in coupling between Cl bridges and Br bridges in Ni(II) dimers (this being the first magnetostructural report on a $[\{NiBr\}_2]^{2+}$ unit), we feel obliged to note that for **1** the average Ni–Br bond length is 2.583 Å, for **2** the average Ni–Cl bond length is 2.436 Å, and these differ by 0.147 Å; this difference is similar to the difference in ionic radii for Br and Cl (0.15 Å). The ferromagnetic coupling is stronger in **1** even though the effective Ni–Br length is the same as the effective Ni–Cl length in **2** and suggests that the extent of ferromagnetic coupling in these complexes depends upon something other than a simple consideration of the length of the superexchange pathway. As mentioned in the Introduction, in cases with significant tetragonal distortions, the greater the distortion, the larger the antiferromagnetic coupling [2]. Perhaps in **1** and **2**, the geometries about the Ni(II) center are sufficiently different from octahedral that the e_g level is no longer truly degenerate, and the distortion is sufficient to weaken the ferromagnetic coupling, but not sufficient to render the coupling antiferromagnetic.

Table 4
Magnetostructural parameters for selected complexes containing $[\{NiX\}_2]^{2+}$.

Compound [a]	J/k	g	D/k	$Z'J'/k$	∠	X1	X2	L	Reference
1	10.0	2.34	1.22	0.06	92.49(4)	2.504(1)	2.662(1)	5.166	this work
$\{Ni(en)_2Br\}_2Br_2$	12.4	2.12	9.5	−0.40	na	na	na	na	[3]
$\{Ni(eg)_2Br\}_2Br_2$	12	2.25		−0.4	na	na	na	na	[4]
$\{Ni(EtOH)_4Br\}_2Br_2$	na	na	na	na	91.0(3)	2.525(3)	2.556(3)	5.081	[9]
2	7.6	2.07	0.51	0.11	87.37(3)	2.3655(8)	2.507(1)	4.872	this work, [10]
$\{Ni(en)_2Cl\}_2Cl_2$	14.2	2.14	9.4	−0.24					[3]
$\{Ni(eg)_2Cl\}_2Cl_2$	13	2.25		−0.3	93.03(5)	2.383(1)	2.383(1)	4.766	[4,24]
$\{Ni(en)_2Cl\}_2Cl_2$	5.0	2.25	14	−0.3	96.55(1)	2.471(1)	2.561(1)	5.032	[5]
$\{Ni(en)_2Cl\}_2Cl_2$	9.57	2.211	5.2		96.6(1)	2.461(3)	2.551(3)	5.012	[6]
$\{Ni(en)_2Cl\}_2(ClO_4)_2$	12.8	2.175	6.0		95.4(1)	2.461(3)	2.512(3)	4.973	[6]
$\{Ni(en)_2Cl\}_2(BPh_4)_2$	13.7	2.162	11.1		95.62(9)	2.403(2)	2.503(2)	4.906	[6,8]
$(C_3H_{12}N_2)_2\{NiCl_4H_2O\}_2$	11.7	2.297	−4.9	−0.76	95.05(5)	2.430(2)	2.459(1)	4.889	[7]

[a] en is ethylenediamine, eg is ethylene glycol. J, g, D, $Z'J'$ are defined in the text. ∠ is the Ni–X–Ni angle in °, X1 is the shorter of the two Ni–X bonds in Å, X2 is the longer of the two Ni–X bonds in Å, and L is the sum of X1 and X2. na is not available. The units for J, D and $Z'J'$ are cm^{-1}.

3.2. Structure in solution

The solution structures for both **1** and **2** were investigated using electronic spectroscopy, ^{1}H NMR spectroscopy and mass spectrometry all using acetonitrile as solvent. In solution, one can envision three obvious possibilities: the dimeric structure dissociates into $[Ni(TPA)X]^+$ units, the dimeric structure dissociates and solvent is added giving $[Ni(TPA)X(solvent)]^+$ units, or the dimeric structure remains intact. The latter interpretation is most consistent with the data, and we interpret the spectroscopy from this perspective.

For **1** in acetonitrile, the electronic spectrum consisted of three major bands at 940, 588 and 304 nm ($\varepsilon = 30.8$, 34.7 and 231 M^{-1} cm^{-1}, respectively), and two minor features at 813 and 452 nm. For **2**, similarly there were three major bands at 957, 591 and 304 nm ($\varepsilon = 22.4$, 23.1 and 537 M^{-1} cm^{-1}, respectively), and one minor feature at 806 nm. The spectrum of **2** is similar to that reported recently [26] for $[\{Ni(TPA)Cl\}_2](ClO_4)_2 \cdot H_2O$ which had features at 955, 592 and 323 nm and remains pseudo-octahedral in CH_3CN solution. The assignments of the three major bands are to the spin allowed d–d transitions typical of Ni(II). The difference in λ_{max} for the lowest energy band indicates that the bromide dimer **1** has a stronger ligand field than the chloride dimer **2**.

For **1** in CD_3CN, the ^{1}H NMR spectrum exhibits five features at 138, 76, 52, 47 and 14 ppm, and **2** exhibits similar features at 140, 71, 53, 46 and 14 ppm. The two most shifted features are extremely broad with the feature near 75 ppm having roughly twice the intensity of the most shifted feature. We assign these features, based primarily upon the distance of the hydrogen atoms from the nickel centers (assuming the σ contact shift mechanism is operable), as follows: 140 (*ortho*), 75 (CH_2), 50 (*meta*), 45 (*meta*), and 15 (*para*), where the terms refer to aromatic ring position relative to the pyridyl nitrogen. The observation of paramagnetic shifting confirms that the species are paramagnetic in solution. There is no evidence of splitting of these features, thus all of the pyridyl rings are in equivalent positions. This equivalence supports the interpretation that the e_g level remains degenerate in solution since significant splitting of this level would be expected to lead to different pyridyl environments (again assuming the σ contact shift mechanism is operable).

For **1** in acetonitrile, key clusters of peaks in the mass spectrum were observed at m/z of 429, 891, 937, 957 and 975. These are assigned as $[\{Ni(TPA)Br\}_2]^{2+}$, $([\{Ni(TPA)Br\}_2]Cl)^+$, $([\{Ni(TPA)Br\}_2]Br)^+$, $([\{Ni(TPA)Br\}_2]ClO_4)^+$, and $([\{Ni(TPA)\}_2Br](ClO_4)_2)^+$, respectively. The feature at 429 is the most intense, with the other features having relative intensities of less than 4% of the main feature. For **2**, key clusters of peaks were observed at m/z of 383, 803, 867 and 931. These are assigned as $[\{Ni(TPA)Cl\}_2]^{2+}$, $([\{Ni(TPA)Cl\}_2]Cl)^+$, $([\{Ni(TPA)Cl\}_2]ClO_4)^+$ and $([\{Ni(TPA)\}_2Cl](ClO_4)_2)^+$. The feature at 383 is the most intense, with the other features also having relative intensities of less than 4% of the main feature. If the main features resulted from dissociation of the Ni dimer to give monomers of formula $[Ni(TPA)X]^+$, rather than our assignment of $[\{Ni(TPA)X\}_2]^{2+}$, and if these monomers were to pick up acetonitrile or water to give six-coordinate species, we would expect to see features at 41 or 18 m/z higher, but such features are not observed. Similarly, one might expect the halide of a five-coordinate monomeric species to be replaced by solvent, but no features corresponding to such species were observed. The additional key clusters of peaks in the mass spectra of **1** and **2** all support the presence of the dimeric species in solution.

4. Conclusions

$[\{Ni(TPA)Br\}_2](ClO_4)_2 \cdot 2HNEt_3ClO_4$ (**1**) is isostructural with the chloro analog (**2**) and contains an asymmetrically dibridged centrosymmetric nickel(II) dimer. The Ni atoms are pseudo-octahedral six-coordinate. These two compounds (**1** and **2**) exhibit ferromagnetic coupling in the solid state with the bromo analog (**1**) more strongly coupled than the chloro analog (**2**). The strength of coupling does not appear to be simply dependent upon the length of the effective ferromagnetic superexchange pathway. The dimeric structures of **1** and **2** persist in solution as evidenced by electronic spectroscopy, ^{1}H NMR spectroscopy and mass spectrometry.

5. Supplementary material

Anisotropic thermal parameters, additional bond distances and angles, hydrogen atom parameters, observed and calculated structure factors, fits of the magnetic susceptibility data, and mass spectral data are available from the authors upon request.

Acknowledgements

We are grateful to the Kresge Foundation for providing the funds for the purchase of the diffractometer used in this work. CJO gratefully acknowledges the support of this work by AMRI through DARPA Grant No. MDA972-97-1-0003.

References

[1] J.C. Jansen, H. van Koningsveld, J.A.C. van Ooijen, J. Reedijk, Inorg. Chem. 19 (1980) 170 and references therein.
[2] K.K. Nanda, R. Das, L.K. Thompson, K. Venkatsubramanian, P. Paul, K. Nag, Inorg. Chem. 33 (1994) 1188.
[3] A.P. Ginsberg, R.L. Martin, R.W. Brookes, R.C. Sherwood, Inorg. Chem. 11 (1972) 2884.
[4] D. Knetsch, W.L. Groenveld, Inorg. Nucl. Chem. Lett. 12 (1976) 27.
[5] K.O. Joung, C.J. O'Connor, E. Sinn, R.L. Carlin, Inorg. Chem. 18 (1979) 804.
[6] Y. Journaux, O. Kahn, J. Chem. Soc., Dalton Trans. (1979) 1575.
[7] C.P. Landee, R.D. Willett, Inorg. Chem. 20 (1981) 2521.
[8] I. Bkouche-Waksman, Y. Journaux, O. Kahn, Transition Met. Chem. 6 (1981) 176.
[9] P. L'Haridon, I. Bkouche-Waksman, J. Inorg. Nucl. Chem. 40 (1978) 2025.
[10] B. Tong, R.E. Norman, S.-C. Chang, Acta Crystallogr., Sect. C 55 (1999) 1236.
[11] A. Altomare, M. Cascarano, C. Giacovazzo, A. Guagliardi, M.C. Burla, G. Polidori, M. Camalli, J. Appl. Crystallogr. 27 (1994) 435.
[12] P.T. Beurkens, G. Admiraal, G. Beurkens, W.P. Bosman, S. Garcia-Granda, R.O. Gould, J.M.M. Smit, C. Smykalla, The DIRDIF program system, Tech. Rep. Crystallography Laboratory, University of Nijmegen, Netherlands, 1992.
[13] D.T. Cromer, J.T. Waber, International Tables for X-ray Crystallography, Kynoch Press, Birmingham, UK, 1974, Table 2.2A.
[14] J.A. Ibers, W.C. Hamilton, Acta Crystallogr. 17 (1964) 781.
[15] D.C. Creagh, W.J. McAuley, in: A.J.C. Wilson (ed.), International Tables for X-ray Crystallography, vol. C, Kluwer, Dordrecht, 1992, Table 4.2.6.10. pp. 219–222.
[16] D.C. Creagh, J.H. Hubbell, in: A.J.C. Wilson (Ed.), International Tables for X-ray Crystallography, vol. C, Kluwer, Dordrecht, 1992, Table 4.2.4.3, pp. 200–206.
[17] TEXSAN, Crystal Structure Analysis Package, Molecular Structure Corporation, The Woodlands, TX, 1985 and 1992.
[18] C.J. O'Connor, Prog. Inorg. Chem. 29 (1979) 203.
[19] A.S. Antsyshkina, M.A. Porai-Koshits, Doklady Chem. 143 (1962) 143. English translation of Doklady Akad. Nauk SSSR 143 (1962) 105.
[20] G.A. Bottomley, L.G. Glossop, C.L. Raston, A.H. White, A.C. Willis, Aust. J. Chem. 31 (1978) 285.
[21] N. Masciocchi, P. Cairati, L. Carlucci, G. Ciani, G. Mezza, A. Sironi, J. Chem. Soc., Dalton Trans. (1994) 3009.
[22] N. Masciocchi, P. Cairati, L. Carlucci, G. Mezza, G. Ciani and A. Sironi, J. Chem. Soc., Dalton Trans. (1996) 2739.
[23] M. James, J. Chem. Soc., Dalton Trans. (1998) 2757.
[24] B.-M. Antti, Acta Chem. Scand. Ser. A 29 (1975) 76.
[25] S.M. Gorun, S.J. Lippard, Inorg. Chem. 30 (1991) 1625.
[26] Z.H. Zhang, X.H. Bu, Z.A. Zhu, Z.H. Jiang, Y.T. Chen, Transition Met. Chem. 21 (1996) 235.